 doi:10.20944/preprints202106.0264.v1

Article

Small oligonucleotides detection in three-dimensional polymer network of DNA-PEG hydrogels.

Alessia Mazzarotta[1], Tania Mariastella Caputo[1], Luca Raiola[1], Edmondo Battista[2] *, Paolo Antonio Netti[1,2,3] , Filippo Causa[2,3]

[1] *Center for Advanced Biomaterials for Healthcare@CRIB, Istituto Italiano di Tecnologia (IIT), Largo Barsanti e Matteucci 53, 80125 Naples, Italy*

[2] *InterdisciplinaryResearch Centre on Biomaterials (CRIB), Università degli Studi di Napoli "Federico II", Piazzale Tecchio 80, 80125 Naples, Italy*

[3] *Dipartimento di Ingegneria Chimica del Materiali e della Produzione Industriale (DICMAPI), University "Federico II", Piazzale Tecchio 80, 80125 Naples, Italy*

* Correspondence: E. B. edmondo.battista@unina.it

Abstract: The control of the three-dimensional (3D) polymer network structure is important for permselective materials when specific biomolecules detection is needed. Here we investigate conditions to obtain a tailored hydrogel network that combine both molecular filtering and molecular capture capabilities for biosensing applications. Along this line short oligonucleotide detection in a displacement assay is set within PEGDA hydrogels synthetized by UV radical photopolymerization. To provide insights on the molecular filter capability, diffusion studies of several probes (sulforhodamine G and dextrans) with different hydrodynamic radii were carried out using NMR technique. Moreover, fluorometric analyses of hybridization of DNA oligonucleotides inside PEGDA-hydrogels shed light on the mechanisms of recognition in 3D, highlighting that mesh size and crowding effect greatly impact of hybridization mechanism onto polymer network. Finally, we found the best probe density and diffusion transport conditions to allow the specific oligonucleotide capture and detection inside PEGDA-hydrogels for oligonucleotide detection and the filtering out of higher molecular weight molecules.

Keywords: PEGDA Hydrogels; 3D recognition; diffusion; strand displacement assay.

1. Introduction

Hydrogels represent a class of polymers of great interest in many field including industrial, biological and biomedical applications. [1-3] Such polymers have a networks which, due to hydrophilic nature, may absorb large amount of water [4-7] and physiological fluids without dissolving. [4, 8-9] The hydrogel network is crosslinked by chemical bond or physical entanglements, which give them the ability to swell or shrink and in general altering the overall structure.[10-14] The knowledge and the control at molecular level of hydrogel structure is then a crucial issue in the network customization to permit the diffusion of specific target, based on the size and the chemical content. In fact, hydrogels can work as molecular filter representing a physical barrier for large molecules and repelling unspecific binding. Furthermore, a specific binding can be achieved adding, during polymerization or in a post modification step, a molecular cue in the bulk or on the surface.

Although hydrogels have been studied for at least three decades, the possibility to exploit the three-dimensional polymeric network as a permselective materials for the detection of specific biomolecular target is still under-explored. In particular, the possibility to exclude interfering biomolecules out form the network could pose the basis for a permselective capture. The three-dimensional structure of hydrogels is best described by three parameters: the polymer volume fraction in the swollen state, $v_{2,s}$, the molecular weight

Preprints (www.preprints.org) | NOT PEER-REVIEWED | Posted: 9 June 2021 doi:10.20944/preprints202106.0264.v1

between crosslinks, ¯;Mc, and the mesh size ξ. The study of these parameters and the suitable modulation to obtain an engineered material, results to be fundamental to understand the network structure that allow us to predict the final properties of our materials. Polymer chain mobility is an important factor governing solute movement within the hydrogel. In general, the diffusivity of a solute through a crosslinked hydrogel decreases as crosslinking density increases, as the size of the solute increases and as the volume fraction of water within the gel decreases.[15] Because of wide application, in the last years several methods have been developed to study bulk hydrogel properties, both theoretically and experimentally.[10-13, 16-26]

Several information can be gained by studying the diffusion of probe molecules through hydrogel networks.[27-29] In the absence of any specific interactions between the probe and the network, the diffusivity of the probe reflects the network structure.[29-31] Common techniques used to study probe diffusion include source–sink techniques,[32] fluorescence recovery after photobleaching (FRAP),[29, 33] and pulsed field gradient-NMR (PFG-NMR).[28, 31, 34-36] The key for PFG-NMR analysis is the fact that NMR data render information on the chemical nature as well as on the molecular mobility of an observed component. This technique has the potential to characterize water binding and mobility in a directly quantifiable manner, and has been commonly used in studies of the water–polymer interaction.[42]

Here we present DNA functionalized PEG crosslinked hydrogels and the investigation of diffusivity of different molecules inside the bulk polymer. The optimizations of crosslinking parameters were carried out with the aim to understand the properties that primarily affect the detection performance of small molecules such as short oligonucleotides inside the polymer network. Indeed, the high concentration of wide range of biomolecules could represent an obstacle for recognition, therefore the possibility to use hydrogels as molecular filter is important to reduce crowding effects within the hydrogels. Therefore, the modulation of both the network structure and capture element density allow to obtain a three-dimensional material for selective target detection. We focus on the synthesis and characterization of PEGDA hydrogels, combining swelling studies with both NMR and fluorometric analysis for diffusion studies. Moreover the fluorometric analyses of the DNA catpure whitin the hydrogels is investigated in details to understand the way to better present the immobilized DNA strand for the capture of its complementary counterpart. In such a way, we were able to optimize the network structure to combine both molecular filter and capture element capabilities to lay the foundation for an engineered hydrogel-based assay for short oligonucleotides from complex media including larger interfering biomolecules.

Preprints (www.preprints.org) | NOT PEER-REVIEWED | Posted: 9 June 2021 doi:10.20944/preprints202106.0264.v1

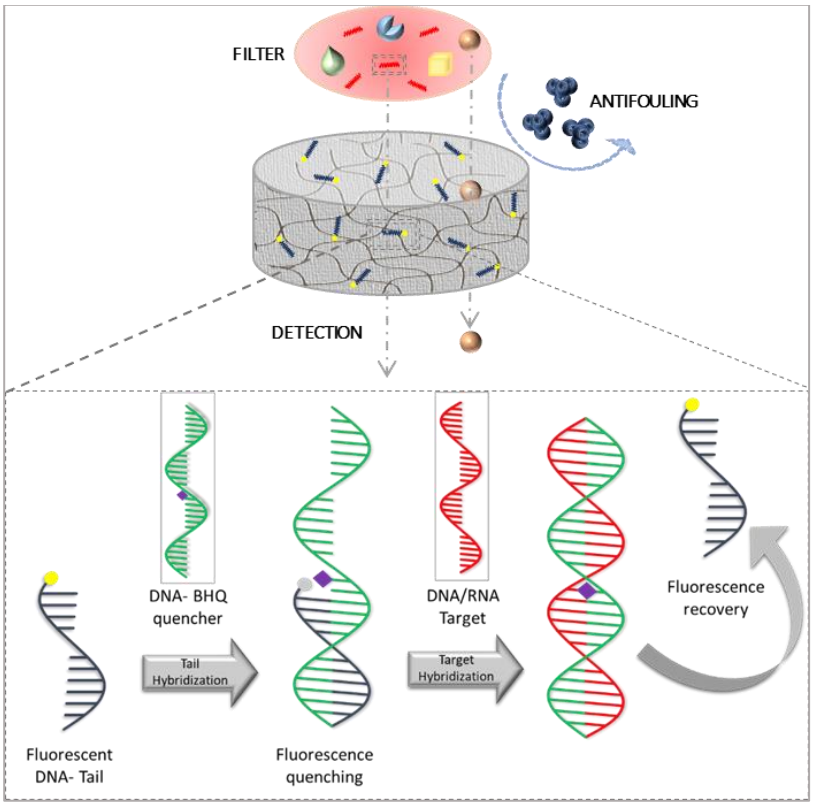

Scheme 1: DNA-PEG Hydrogels with antifouling and permselectivity toward high molecular wheight interefering molecules. In the lowe part of the scheme the oligonucleotide detection system implemented in the DNA-PEG hydrogels: Fluorescent DNA-tail (T-DNA) immobilized in the hydrogel is partially hybridized with a longer complementary DNA-BHQ quenching strand; in presence of DNA or RNA target the displacement brings the formation of the hybridized DNA-BHQ/DNA or RNA target, with recovery of fluorescence inside the hydrogel.

2. Results and Discussion

The bulk-hydrogels were synthesized using a UV free radical photopolymerization. The process involves three basic steps (**Figure 2**a). First, a free radical must be formed through the initiation step. For the PEGDA system used in this work, the initiator is DAROCUR1173, which forms a free radical under UV light (**Figure 2**-a). The next step is known as propagation, where the free radical from the initiator comes into contact with the end of a PEGDA molecule and reacts with the carbon-carbon double bond in the acrylate functional group (**Figure 2**-b). This step produces a second free radical species, which can go on to react with more PEGDA polymers propagating the crosslink. The final step in the process of this polymerization is the termination, which occurs when two radical species meet and bonds form between them. A general reaction scheme for difunctional monomers in a radical polymerization forming a crosslinked network is reported (**Figure 2**-c). In the case of DNA-PEG hydrogels, oligonucleotides are polymerized starting from methacrylate strands and treated in the same way as PEGDA hydrogels.

Preprints (www.preprints.org) | NOT PEER-REVIEWED | Posted: 9 June 2021 doi:10.20944/preprints202106.0264.v1

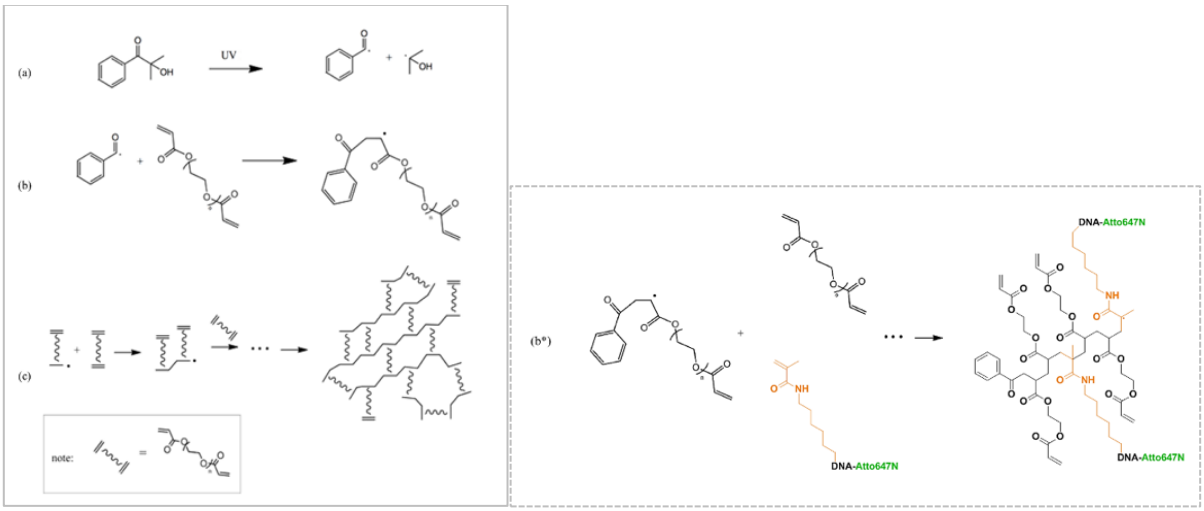

Figure 2: UV free radical photopolymerization: (a) Initiation mechanism, (b) Propagation mechanism, (c) Formation of a cross-linked polymer network (b*) UV free radical photopolymerization between PEGDA and methacrylate oligonucleotide

In Figure 2 is shown H^1-NMR spectra of the PEGDA-Hydrogels soon after the cross-linking. The complete polymerization was confirmed by the disappearing of the PEGDA acrylic signals (region 6 to 6.6 ppm, See Supp Info Figure S1). In addition, the very broad peak from 4.5 to 3.5 ppm showed the transition of PEG chains from a very flexible situation (solution) to a less flexible state of cross-linked chains. Relative decrease of the DAROCUR 1173 peak intensities also confirmed that a large amount of the initiator was consumed in the polymerization reaction. The broad peak at 4.65 ppm is the H_2O residual signal. One-dimensional ^{1}H-NMR spectra of PEGDA/DAROCUR 1173 solutions were recorded before and after UV treatment and all the comparison of the different components are reported in supplementary information (Fig S1 and Fg S2).

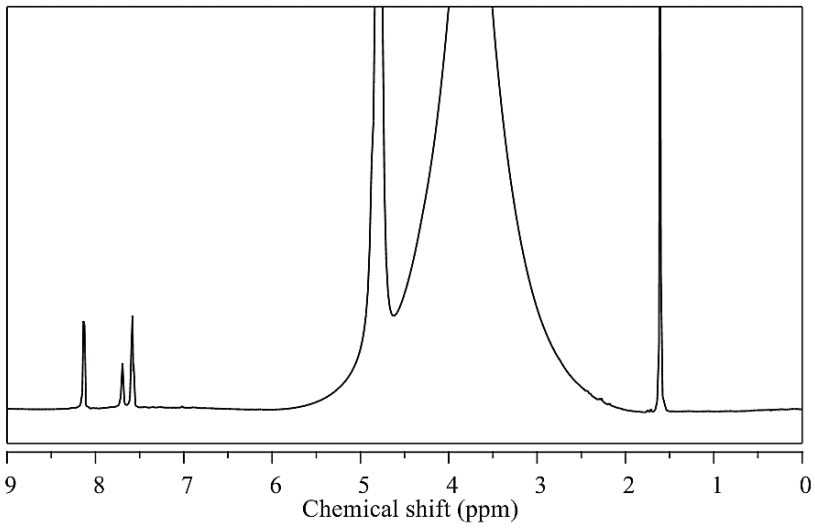

Figure 2**:** ^{1}H-NMR spectrum of PEGDA/darocur solution after polymerization.

Preprints (www.preprints.org) | NOT PEER-REVIEWED | Posted: 9 June 2021 doi:10.20944/preprints202106.0264.v1

Molecular parameters of the three-dimensional network

The swelling ratio and polymer volume fraction in the swollen state can be measured through equilibrium swelling experiment.[13] Then the molecular weight and the mesh size can then be obtained by a theoretical model for swelling of polymer hydrogels.[27] Indeed, the structure of hydrogels can be analyzed by the Flory-Rehner theory, subsequently modified by Peppas and Merrill, which developed a theoretical framework that has significant success in describing the hydrogel swelling behaviour.[10, 18]

Cylindric PEGDA hydrogels of 1 cm height and 1 cm in diameter were prepare at different polymer concentration (10-15-20-25-30 % w/v) to obtain various network structure with different molecular filter capability. Water content was experimentally measured by gravimetry (F_{water}) and all fundamental swelling parameters derived ($v_{2,s}$, Q, $\bar{}$;M_c , ξ) for each preparation and summarized in Table 1.

Table 1: Properties of bulk hydrogels of PEGDA. All values were calculated from averaged measured values.

	PEGDA 10%	PEGDA 15%	PEGDA 20%	PEGDA 25%	PEGDA 30%
F_{water}	91.2% ± 0.1%	87.2% ± 0.1%	82.7% ± 0.1%	78.2% ± 0.1%	73.5% ± 0.1%
$v_{2,s}$ ($\cdot 10^{-3}$)	79.2 ± 0.9	116.2 ± 1.8	157.5 ± 0.5	199.3 ± 0. 5	243.4 ± 0.4
Q	12.63 ± 0.14	8.61 ± 0.14	6.349 ± 0.018	5.017 ± 0.012	4.109 ± 0.008
$\bar{}$;M_c (Da)	340.43 ± 0.21	329.35 ± 0.66	311.62 ± 0.23	288.24 ± 0.30	259.06 ± 0.31
ξ (nm)	2.652 ± 0.011	2.299 ± 0.014	2.022 ± 0.003	1.800 ± 0.002	1.597 ± 0.002

First water content ranges from 91% up to 73% with increasing of polymer concentration. Changing the PEGDA concentration, polymer volume fraction results in the range of 0.08-0.24. As expected, Q, $\bar{}$;M_c and ξ decreased with increase of polymer concentration. In fact, the equilibrium-swelling ratio decreased from 12.6 to 4.1 as the crosslinking density increased. The molecular weight between crosslinks decreased from 340 to 259 Da as the percent polymer fraction increased from 10 to 30% (w/v). Moreover, mesh size (ξ) linearly decreases with the increase of polymer fraction ranging from 2.6 in the case of 10% up to 1.6 nm in the case of 30% (Fig. S3). These results confirm that the polymer concentration permit to optimize the network density as well as the mesh size for the specific purpose.

NMR: diffusion studies

The NMR allows to gain information on the on the molecular mobility of an observed component. The advantage of this analysis is that works in the absence of concentration gradients, studying instead the chaotic motion of molecules driven by intermolecular collisions.[28] Diffusion times over a large range, usually from few milliseconds up to seconds, are available via PFG-NMR techniques and can be chosen arbitrarily by selecting the correct attenuation parameters.[28] The study of the probe diffusion on these short timescales, allow obtaining much information on the microscopic structure of materials.[28, 37-41] In particular, we are interested in measuring the water self-diffusion coefficient (D) that is directly related to the potential for water to leave a hydrogel.[42]

DOSY experiments were used to study the diffusion of molecules, with different size, in hydrogels samples prepared with a PEGDA concentration of 10%, 15% and 20% (w/v). Firstly, we evaluated the water self-diffusion coefficient. Measurement resulted to be 24.55 ± 0.11 ($\cdot 10^{-10}$ m^2/s), in agreement with literature data.[46] Furthermore, diffusion coefficient of solvent in the first hydration shell of hydrogels sample was calculated. Results indicated that water diffusion coefficient was affected by the PEGDA concentrations as shown in Fig S7 (Fitting curve reported in Supp. info).

Moreover, several probes were properly chosen to simulate the behavior and diffusion of biological molecules. In particular, the smallest dextran (3 kDa) has hydrodynamic

Preprints (www.preprints.org) | NOT PEER-REVIEWED | Posted: 9 June 2021 doi:10.20944/preprints202106.0264.v1

radius comparable with oligonucleotide (that represent molecule that we want to capture). On the other hand, 40 kDa dextran and blood proteins, such as albumin, have similar hydrodynamic radii and represent molecules that should be excluded out from the network. In order to validate our choice, hydrodynamic radii of sulfo-rhodamine G and dextrans (3 kDa, 10 kDa, 40 kDa) were calculated using Einstein-Stokes equation. Results reported in **Table 2** showed that probes diffusion coefficients in D_2O (D_0) were in the range of 0.5-3.7 [10^{-10} m^2/s] and their hydrodynamic radii had values between 3.9 and 0.6 nm. These molecules had a size comparable with the range between small oligonucleotides and large molecules. Afterwards, probes diffusion coefficients in bulk hydrogels (10%, 15%, 20% w/v) were calculated, as reported in **Table 2**. Diffusion coefficient of small molecules, as sulforhodamine G (SR-G), should not be affected by a very large network structure and their values should be comparable with free diffusion of probe in water.[3] On the other hand, for high molecular weight molecules such as dextrans we expect a decreasing trend of diffusion coefficient values from the water solution to the highest polymer percentage hydrogel.

Table 2: Self diffusion (D_0 [$\cdot 10^{-10}$ m^2/s]), hydrodynamic radii (R_0 [nm]) and diffusion coefficient ($\cdot 10^{-10}$ m^2/s) of water and different probes in both water and PEGDA hydrogels.

	D_0	R_0	D PEGDA 10%	D PEGDA 15%	D PEGDA 20%
Water	24.55 ± 0.11	0.09 ± 0.01	18.84 ± 0.03	16.05 ± 0.02	15.08 ± 0.13
Sulforhodamine G	3.67 ± 0.06	0.61 ± 0.01	3.14 ± 0.15	3.11 ± 009	3.10 ± 0.24
Dextran 3kDa	1.60 ± 0.03	1.34 ± 0.01	0.87 ± 0.12	0.63 ± 0.02	0.46 ± 0.04
Dextran 10kDa	0.91 ± 0.01	2.41 ± 0.01	0.27 ± 0.02	0.234 ± 0.001	0.120 ± 0.005
Dextran 40kDa	0.557 ± 0.008	3.92 ± 0.03	0.160 ± 0.001	0.140 ± 0.008	0.557 ± 0.008

Moreover, the effect of the polymer concentration on the reduction of diffusion coefficients was highlighted in **Figure 3** where D/D_0 was plotted against polymer concentration. D/D_0 values of water and sulforhodamine G, the smallest probe. It resulted to be constant (~85%) for all PEGDA concentrations; by the contrast, dextrans probe showed a significant mobility reduction, related with the polymer concentrations. In particular, for 3 kDa dextran, D/D_0 decreased from 55 % in the wider network up to 30% in the tighter one. Instead, both 10 kDa and 40 kDa had similar trend, between 30% and 15%. This confirms the mobility of these bigger molecules deeply affected by the polymer network.

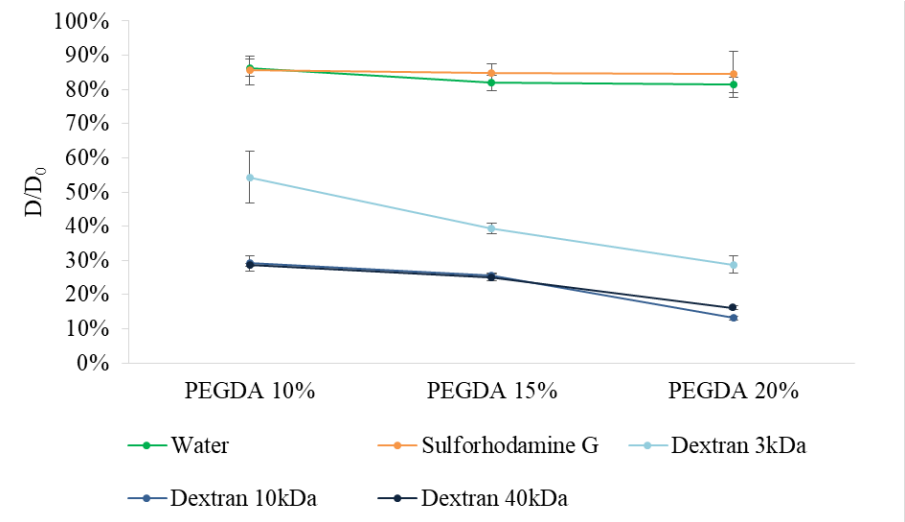

Figure 3: Effect of the polymer concentration on the reduction of diffusion coefficients (D/D_0).

Preprints (www.preprints.org) | NOT PEER-REVIEWED | Posted: 9 June 2021 doi:10.20944/preprints202106.0264.v1

NMR analyses show that hydrogels with different PEGDA concentrations are able to largely impair molecules trafficking because of their low diffusion coefficient. However, we can modulate the diffusion of the probe modifying the mesh size of the network, changing the PEGDA concentrations. In particular, Dextran 3 kDa are capable to diffuse through all the networks while Dextrans 10 kDa and 40 kDa showed a very low mobility also in the network with largest molecular mesh.

Assay set-up

Preliminary studies for the detection assay optimization were performed using a probe scheme already tested in previous work of our group.[47] An overview of probe mechanism is reported in **Scheme 1** (lower part) where fluorescent T-DNA is a short fluorescent DNA tail (12 nt), labelled at 5′ end with ATTO 647N and modified at 3′ with methacrylamide spacer to allow its covalent binding with polymer network. A Quencher strand (21 nt), internally modified with a Black Hole Quencher (BHQ), was used as probe diffusion. When the tail hybridizes, the BHQ comes in close proximity with the fluorophore and fluorescence quenching occurs (for sequence and thermodynamic parameters see Sup. Info). Here we probed the quenching effect due to the partial hybridization of the T-DNA, immobilized in the hydrogel, and the quencher strand BHQ. After an appropriate optimization we tested the efficiency of quenching on DNA-PEG hydrogels obtained with 5 μM T-DNA co-polymerized (see Figure S8). We reported the fluorescence intensity for the upper and lower polymer concentration (20% and 10% (w/v)). We added BHQ strand and repeated the analysis. Comparing values of quenching percentage for the two different polymer concentrations, we obtained a similar quenching (~75%). After a washing of the bulk with PBS buffer, we report a high recovery of fluorescence (above 95%) for PEGDA 20% bulk. In that case, the quenching was only transient even after a second repetition of the quenching step. In this case, in fact, the BHQ-strand diffuse in the bulk and comes in proximity with the fluorophore. This is the case of dynamic quenching (**Figure 4a**). Here the correct hybridization does not occur to form a stable double strand while the quenching strand comes near enough to collide with fluorophore with a consequent fluorescence decrement. By the contrast, in PEGDA 10%, the network was sufficiently wider to allow the formation of stable complex between oligonucleotide strands, so that the tail and quencher came in proximity. In this case quenching effect is shown and the partial hybridization occurred to form a stable duplex even after several washes (**Figure 4b**). The formation of the DNA duplex imply that the two interacting molecules (T-DNA and BHQ-strand, in this case) are in the correct orientation to form the hydrogen bonds between the complementary bases. The tight mesh size could provide a limited space and a stiffening of the structure. Both effects could, in turn, limit the degree of freedom of the immobilized molecules to explore the space and assume the right orientation for the formation of the hydrogen bonds.

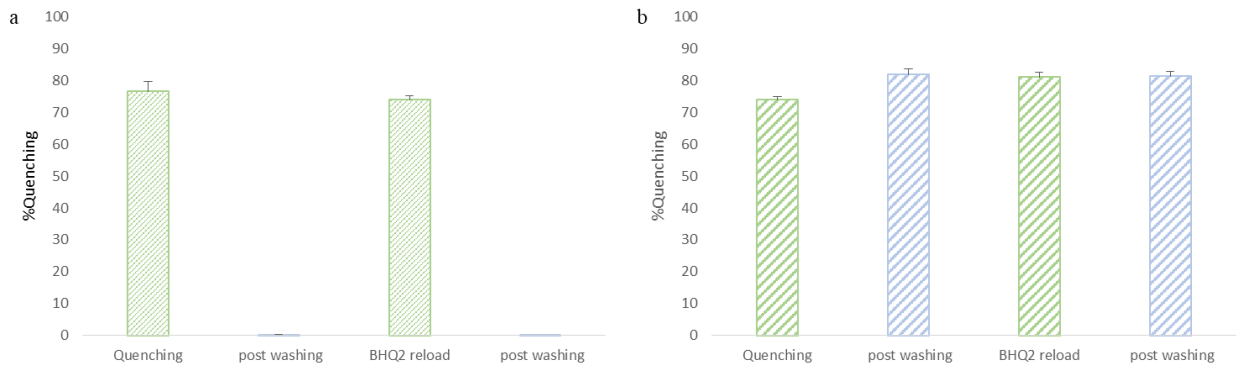

Figure 4: Quenching efficiency of ATTO-BHQ in PEGDA 20% (a) and 10% (b), by using 5 μM of BHQ strand.

Preprints (www.preprints.org) | NOT PEER-REVIEWED | Posted: 9 June 2021 doi:10.20944/preprints202106.0264.v1

To prove such hypothesis we tested a 50% DNA-PEG hydrogels using both complementary (C) and non-complementary (N) BHQ-probes. As reported in Figure 5, after the addition of C-BHQ we obtained a ~70% quenching that strongly decreased at ~3% after washing. This result is also confirmed by adding a not complementary strand N-BHQ. In this case despite the increase of quenching with N-BHQ amount up to 10 fold, we found a huge recovery of the fluorescence after washings. Therefore, we can conclude that both tight mesh size and high concentration of T-DNA inside the bulk do not allow for an effective duplex hybridization even at high BHQ-strand concentrations.

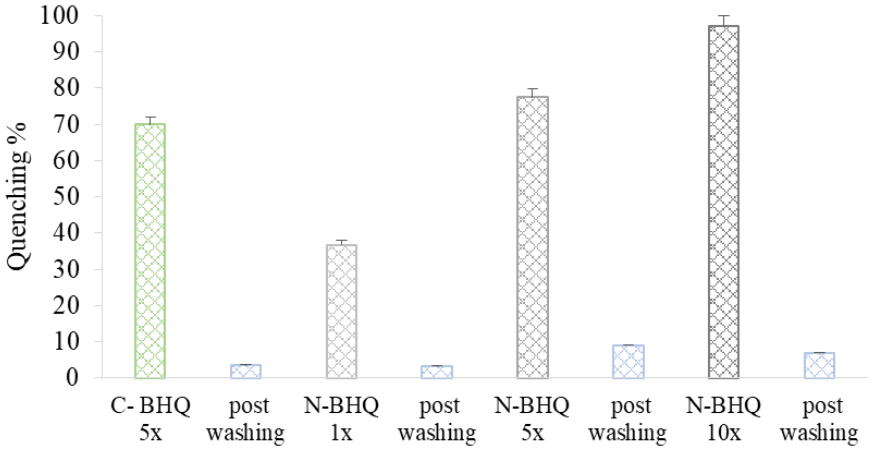

Figure 6: Quenching efficiency with complementary strand (C-BHQ) in green and not complementary strand (N-BHQ) in grey at different concentrations.

We also investigated the effect of the mesh size and density of functionalization with T-DNA by following the kinetic of hybridization of the BHQ-strand over long time (120hrs). All tests were carried out with 1 μM and 5 μM F-DNA-Tail with BHQ-strand 1x and 5x with respect to the nominal T-DNA density.

Preprints (www.preprints.org) | NOT PEER-REVIEWED | Posted: 9 June 2021 doi:10.20944/preprints202106.0264.v1

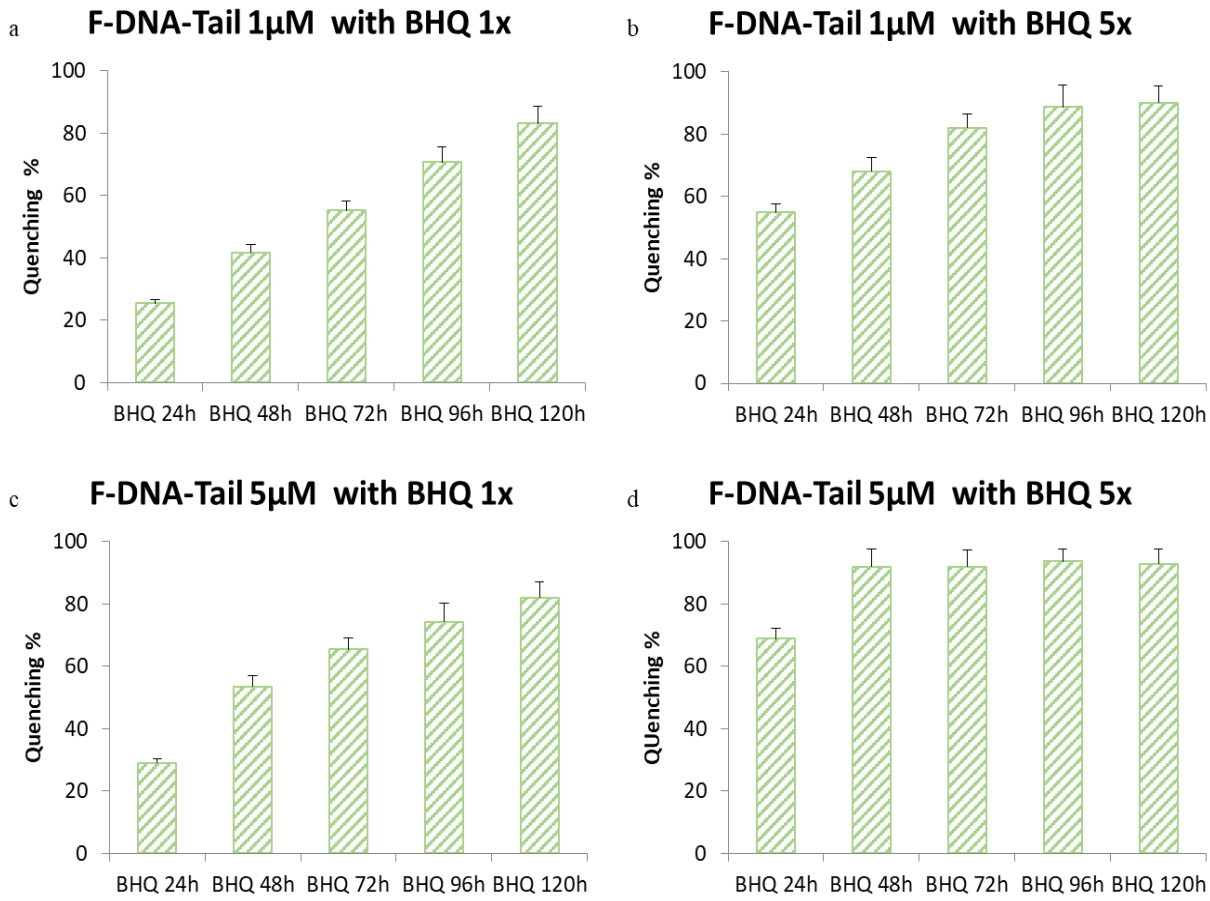

Figure 4: Quenching kinetic in PEGDA 10% with several oligonucleotides concentrations: (a) F-DNA-Tail 1µM- BHQ 1x; (b) F-DNA-Tail 1µM- BHQ 5x; (c) F-DNA-Tail 5µM- BHQ 1x; (d) F-DNA-Tail 5µM- BHQ 5x.

As regards PEGDA 10%, **Figure 4** showed that quenching percentage increased with increasing of both T-DNA and BHQ concentrations. In the case of T-DNA 1µM with BHQ in 1x (Figure 7a), we see a linear increase of quenching up to 80% after 120h. Further increase of quenching strand (BHQ 5x) (Figure 7b) brings a quenching efficiency of about 80% after 72hrs. After 120hrs the efficiency of quenching was above 90%. Increasing the concentration of T-DNA at 5µM with brings to a slight acceleration of quenching for the lower BHQ (figure 7c), while the increase to BHQ 5x (figure 7d) produce a quenching efficiency above 90% after only 48hrs.

On the other hand, for PEGDA 15%, only in the case of T-DNA 5 µM and BHQ 1x was possible to reach, after 96h, an 80% quenching (figure 8b). In fact, at constant T-DNA, a lower concentration BHQ 1x was not enough to provide a good quenching, while an increase of T-DNA hinders the effective hybridization.

Preprints (www.preprints.org) | NOT PEER-REVIEWED | Posted: 9 June 2021 doi:10.20944/preprints202106.0264.v1

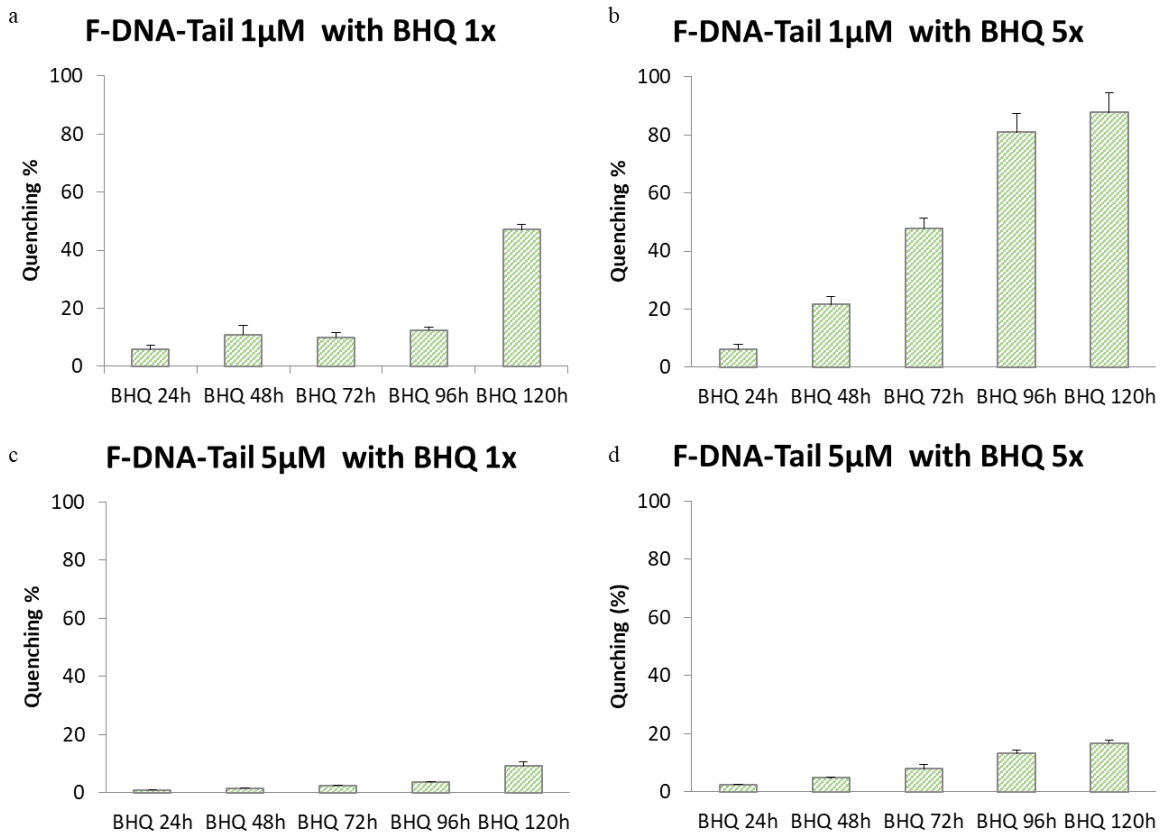

Figure 5: Quenching kinetic in PEGDA 15% with several oligonucleotides concentrations: (a) F-DNA-Tail 1µM- BHQ 1x; (b) F-DNA-Tail 1µM- BHQ 5x; (c) F-DNA-Tail 5µM- BHQ 1x; (d) F-DNA-Tail 5µM- BHQ 5x.

Finally, for PEGDA 20% we reached very low values of quenching for all sample preparations (Figure 9). In this case the efficiency of quenching does not reach more than 10% and the effect of mesh size and density of functionalization is more evident in the obstruction of free diffusion of quenching molecules. Moreover, the decrease of quenching percentage post-washing confirmed the not efficient hybridization (data not shown).

Overall, such observations are useful to define the behavior of functionalize hydrogels for the direct capture of oligonucleotides.

Preprints (www.preprints.org) | NOT PEER-REVIEWED | Posted: 9 June 2021 doi:10.20944/preprints202106.0264.v1

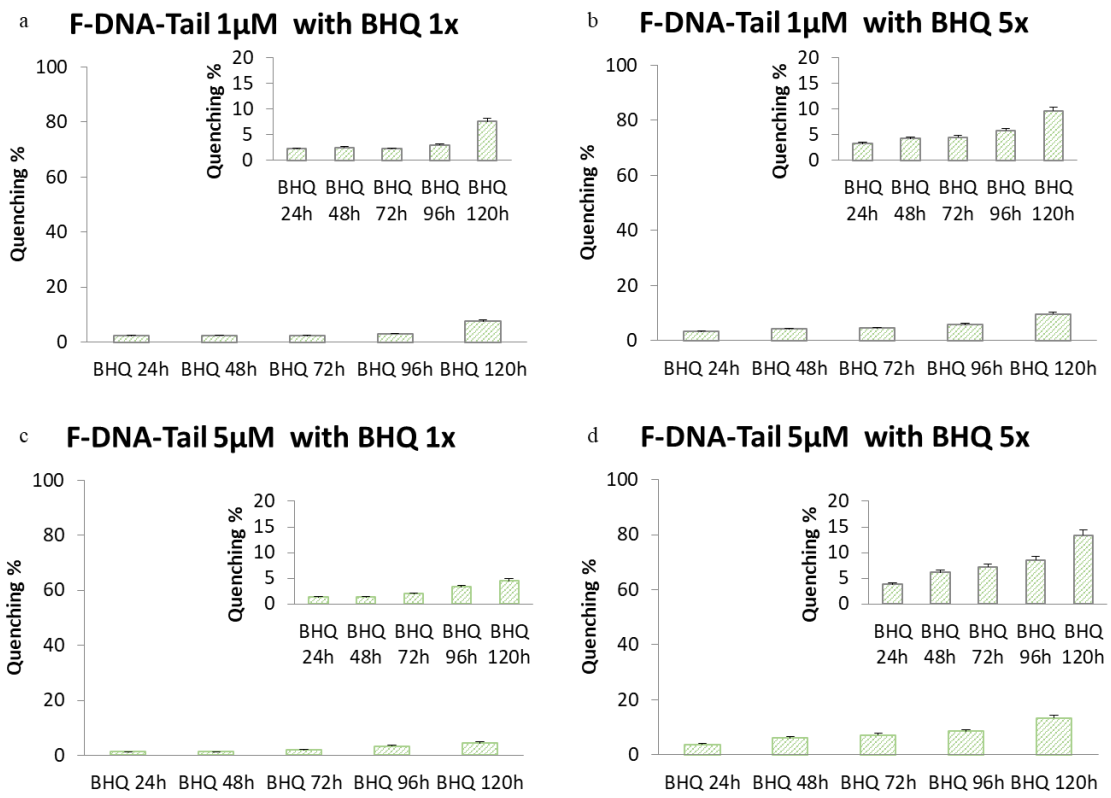

Figure 6: Quenching kinetic in PEGDA 20% with several oligonucleotides concentrations: (a) F-DNA-Tail 1µM- BHQ 1x; (b) F-DNA-Tail 1µM- BHQ 5x; (c) F-DNA-Tail 5µM- BHQ 1x; (d) T-DNA 5µM- BHQ 5x.

In order to provide insight on the possibility to use such design for a displacement assay we proceed to test the capability of DNA-PEG hydrogels to serve as selective sponges. We added the target to for each polymer concentrations with density of functionalization of 1µM and 5µM. The analysis was performed for all bulk hydrogels tested for quenching. All tests were carried out with Target concentration 10x with respect of T-DNA immobilized and the fluorescence recovery was measured taking as reference the quenched level. **Figure 7**.

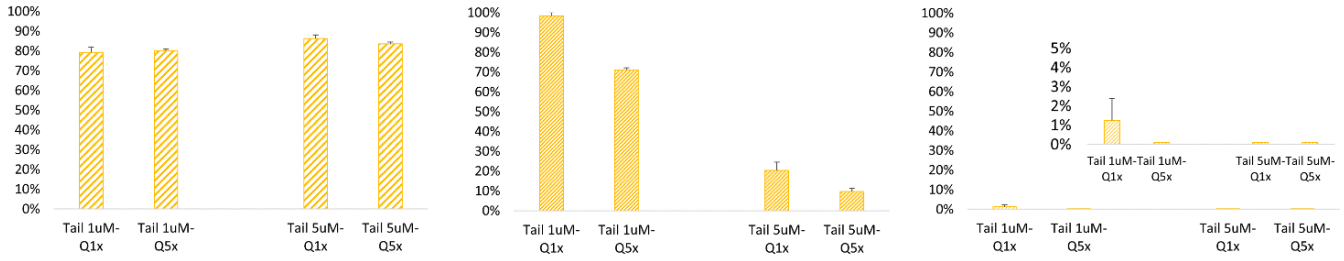

Figure 7: Fluorescence recovery after displacement with 10X Target-DNA in DNA-PEG hydrogel 10% (I) – 15% (II) and 20% (III) with Tail concentrations of 1µM and 5µM.

At first glance the 10% DNA-PEG hydrogels produced a high recovery of fluorescence in all cases. In the case of 15% a drop in recovery of fluorescence is observed at higher density of functionalization, while for 20% DNA-PEG hydrogels the recovery is very poor.

Overall, these results confirm that higher polymer concentration produce a crowding effect that reduce molecular mobility inside the hydrogel and at same time a stiffening of the network that reduce the flexibility of the capturing DNA tail. Polymer concentrations

 doi:10.20944/preprints202106.0264.v1

higher than 15% of PEGDA were not suitable for probe diffusion resulting slow down even for small molecules (below 3KDa). In this case to observe a recognition in 3D resulted more effective a reduction in polymer concentration and density of functionalization. The results presented make the recognition in 3D a complex balance between the mesh size, the stiffness of the substrate and the density of functionalization. As observed here the reduction of mesh size provide the space for the diffusion of small oligonucleotides even though the reduced mobility of the capture molecules does not allow for proper hybridization.

3 Conclusions

In this paper, we focused on the development of PEGDA-based bulk hydrogels for perm-selective detection of small DNA oligonucleotides (21bp). Swelling characterization showed the possibility of modulating mesh size by changing the polymer concentration. This is the case to achieve filtering capability of the 3D hydrogels with regards of high molecular weight molecules.

NMR analysis confirmed the opportunity to use hydrogels as molecular filter. In particular, 10% and 15% polymer concentrations resulted suitable to be used as molecular filters with cut-off of radius of 2.4 nm comparable to the mesh size. In fact, these networks allowed the diffusion of molecules with size comparable with our probe (oligonucleotides) and excluded larger molecules with size similar to proteins and antibody.

Moreover, fluorometric analysis gave us important information regarding the ratio between polymer and oligonucleotides concentrations to obtain an efficient hybridization. In particular, 10% and 15% PEGDA concentrations showed a suitable network for both oligonucleotide diffusion and effective hybridization. In addition, results showed that for 10% of polymer we can obtain a good quenching percentage also for the highest oligo concentration. On the other hands, for 15% of polymer, we cannot use oligonucleotide concentration higher than 1 μM, because of crowding effect.

In conclusion, our results showed the possibility to obtain functionalized and engineered materials, with a tunable network, that allow to combine both molecular filter and capture element capabilities. In this way, we can improve these materials to simplify the detection analysis of several target.

4. Materials and Methods

Materials and reagents

Poly(ethylene glycol)diacrylate (PEGDA-700 Da), Deuterium oxide (D_2O), Sulforhodamine G, Ethanol and Diethyl ether were purchased from Sigma-Aldrich (St. Gallen, CH) and used as received. Crosslinking reagent 2-Hydroxy-2-methylpropiophenone (DAROCUR 1173, CIBA) was provided from Ciba. Texas Red labelled dextrans with different molecular weight (3 kDa, 10 kDa and 40 kDa) were supplied by Thermo Fisher Scientific. DNA oligonucleotides were purchased from Metabion with HPLC purification. NMR tubes, properly designed for gel samples, were supplied by New Era Enterprises, Inc and OptiPlate-96 F HB were purchased by PerkinElmer.

Synthesis of bulk-hydrogel

The hydrogels used here were synthesized by UV free radical polymerization using poly(ethylene glycol) diacrylate (PEGDA, 700 Da), at different concentrations in Milli-Q water and DAROCUR 1173 used as initiator. Each hydrogel sample was prepared dissolving photoinitiator in 10 mL of polymer solution, obtaining an initiator final concentration of ~0.1% v/v. The reaction mixture was strongly mixed and then purged with high purity nitrogen for 5 minutes to remove the excess of oxygen that may interfere with the free radical polymerization. The reaction mixture was then carried out in 10 mL test tubes and illuminated with UV lamp (λ = 365 nm and power-lamp = 10 W) for 5 minutes leading to complete polymerization. For NMR studies, we reduced the total reaction volume to 1 mL of deuterated water. Polymerization was performed directly in special NMR tubes

Preprints (www.preprints.org) | NOT PEER-REVIEWED | Posted: 9 June 2021 doi:10.20944/preprints202106.0264.v1

designed for gel samples. Hydrogel samples were than expelled from the NMR tube and put in a solution of D_2O for the next 24h to remove all the unreacted materials. Hydrogels were dried in oven at 30°C for few hours, swelled with 1 mL of probe solution and finally put in the NMR tube for the measurement. In particular, different probes, sulforhodamine G and several dextrans (3 kDa, 10 kDa and 40 kDa) were dissolved in D_2O to reach a final concentration of 1 mg/mL. Moreover, functionalized bulk were synthesized using UV free radical photopolymerization between PEGDA and oligonucleotide, properly modified with methacrylamide moieties. Propagation step of the reaction between polymer and methacrylate oligonucleotide is highlighted in Figure 1b*.

Several recipes with different PEGDA and oligonucleotide concentrations were prepared and tested. The mixture was composed of PEGDA (MW 700 Da) at different concentrations (10-15-20% w/v) in buffer solution, DAROCUR 1173 as initiator and fluorescent oligonucleotide methacrylate (F-DNA-Tail) at different concentrations (1µM-5µM). Our buffer solution was obtained adding 1 x PBS and NaCl 200 mM in milliQ water. The reaction mixture was strongly mixed and then purged with high purity nitrogen for 5 minutes to remove the excess of oxygen that may interfere with the free radical polymerization. Then, 100µL of the mixture was carried out in 96-optiplate, illuminated with the same UV lamp used before for 5 minutes leading to complete polymerization.

Bulk-hydrogel characterizations

Several characterization, attained due to NMR and fluorimeter measurements,were accomplished on different bulk samples to define the structural and diffusion properties of these materials in both PEG-bulk and functionalized-hydrogels.

The *swelling characterization* of hydrogels were carried out applying the equilibrium swelling theory, also known as Flory-Rehner theory. The theory is based on the following equation that allows to calculate the molecular weight between crosslinks that represent a measure of the degree of crosslinking of the polymer. Obviously, due to the random nature of the polymerization process itself only average values of $\bar{}$;M_c can be calculated Eq.1.

$$\frac{1}{\overline{M_c}} = \frac{2}{\overline{M_n}} - \frac{\left(\frac{\bar{v}}{V_1}\right)\left[ln\left(1-v_{2,s}\right)+v_{2,s}+\chi_1 v_{2,s}^2\right]}{\left(v_{2,s}^{1/3}-\frac{v_{2,s}}{2}\right)} \qquad \text{Eq.1}$$

In this equation $\bar{}$;M_n is the molecular weight of the polymer chains prepared in the absence of a crosslinking agent, $v_{2,s}$ is the polymer fraction in the swollen state, $\chi_{1,2}$ is the polymer-solvent interaction parameter, $\bar{}$;ν is the specific volume of the polymer, and V_1 is the molar volume of water.

To apply this equation, several parameters are needed: interaction parameter PEG/water, χ=0.426[43]; specific volume, v=0.91 ml/g; molar volume of water, V1= 18.1 ml/mol [43]; uncrosslinked molecular weight of PEG, M_n = 700 Da [48-50]. Polymer volume fraction in the swollen state ($v_{2,s}$) characterizes how well the polymer absorbs water. It can be expressed as the ratio of the volume of dry polymer, V_d, to the volume of the swollen polymer gel, V_s, and is the reciprocal of the degree of swelling, Q.[44] Here we calculated $v_{2,s}$ using Eq. 2 above.

$$v_{2,s} = \frac{V_d}{V_s} = \frac{1}{Q} = \frac{1}{1+\frac{\rho_{polymer}}{\rho_{solvent}}\left(\frac{m_s}{m_d}-1\right)} \qquad \text{Eq.2}$$

Masses in both conditions were determined as follow: once polymerized, hydrogels were removed from the glass tubes, uniformly cut into samples of short cylindrical shape (1cm height, 1 cm diameter) and then immersed in an excess of milli-Q water in order to remove the unreacted reagents. Water was changed several times for the next 24 h and samples were then swollen overnight in water at room temperature. Then cylindrical parts were gently wiped with a filter paper and weighted to obtain the mass of swollen hydrogel (m_s). For dried measurement, in order to obtain a total dehydration, hydrogels were properly grinded and lyophilized overnight, so the mass of dry samples were recovered (m_d). Therefore, we were able to determine hydrogel volume in both swollen and dry

Preprints (www.preprints.org) | NOT PEER-REVIEWED | Posted: 9 June 2021 doi:10.20944/preprints202106.0264.v1

state applying Eq.2. Moreover, we evaluated the water contents of the gels, which represent the mass fraction of water (F_{water}) in the swollen condition using Eq.3

$$F_{water} = \frac{m_{swollen} - m_{dry}}{m_{swollen}} \quad \text{Eq.3}$$

Once M_c was calculated, the mesh size (ξ) can be determined from the following equation [15]:

$$\xi = v_{2,s}^{-1/3} (\bar{r}_0^2)^{1/2} \quad \text{Eq.4}$$

Where $\bar{r}_0^2$ is the value of the end-to-end distance of PEG chains in the unperturbed state and it is calculated applying Eq.5 :

$$(r_0^2)^{1/2} = C_n N l^2 \quad \text{Eq.5}$$

where C_n is the Flory characteristic ratio, l is the length of each link and N, the number of links in the chain, is given by Eq.6:

$$N = \frac{2\bar{M}_c}{M_r} \quad \text{Eq.6}$$

Where M_r is the molecular weight of the repeating unit of the polymer.

NMR analysis was performed using an Agilent 600 MHz (14 Tesla) spectrometer equipped with a DD2 console. ^{1}H-1D-NMR spectra were recorded at 300 K with 64 scans to obtain a good signal to noise ratio. Diffusion spectra were recorded at 300 K using a Dbppste (DOSY bipolar pulse pair stimulated echo) pulse sequence[45]. An array of 15 pulse field gradient values from 0:98 to 63:7 Gauss/cm were used with a gradient pulse length (δ) of 2 ms. Diffusion delay (Δ) in ms was optimized for each sample to obtain a ratio of 1:0.2 between I(Gmin) and I(Gmax), where I(Gmin) is the intensity of the NMR peak at the minimum gradient value and I(Gmax) is the intensity of the NMR peak at the maximum gradient value. Diffusion coefficients were calculated using the formula reported in Equation 7:

$$I(\delta, \Delta) = I_0 \, exp\left[-D\gamma^2 g^2 \delta^2 \left(\Delta - \frac{\delta}{3}\right)\right] \quad \text{Eq.7}$$

where I and I_0 are the spin echo amplitudes in the presence and in the absence of a magnetic field gradient pulse, respectively; γ is the gyromagnetic ratio of the given nucleus, Hz/T, and g is the magnetic gradient, T/m. NMR data were processed and analyzed using VNMRJ4 software.

*Fluorescence analysis. T*he best concentration of both polymer and oligonucleotide was evaluated and the effective hybridization of Fluorescent-DNA-Tail and BHQ-strand checked. Fluorescence spectra of fixed amount of labelled oligonucleotides were collected in a 1 cm path length cuvette with a Horiba JobinYvon model FluoroMax-4 fluorometer equipped with a Peltier temperature controller. The conjugated and unconjugated sequences were excited at 647 nm with a slit width of 5 nm, and emission spectra were collected from 667 to 750 nm with a slit width of 5 nm. Then, hydrogel bulks were synthetized into optiplate 96 F and analysed by the means of a 2300 EnSpire multilabel reader (Perkin-Elmer, Waltham, MA) . Fluorescence was measured from the top of the plate, with excitation wavelength of 647 nm, and emission wavelength at 667nm, height 9mm and 500 number of flash.

 doi:10.20944/preprints202106.0264.v1

Supplementary Materials: The following are available online at www.mdpi.com/xxx/s1, Figure S1: ^{1}H-NMR spectrum of PEGDA/*DAROCUR 1173* solution before polymerization with signal attribution and related peak integration; Figure S2: ^{1}H-NMR spectra of individual components DAROCUR 1173 (IV) and PEGDA (III) and mixture pre (II) and post-polymerization (I); Figure S3: Mesh size values for different bulk-PEGDA concentrations; Figure S4: NMR- DOSY for water diffusion in PEGDA 10%; Figure S5: NMR- DOSY for water diffusion in PEGDA 15%; Figure S6: NMR- DOSY for water diffusion in PEGDA 20%; Figure S7: 2D DOSY of water (4.645 ppm) in hydrogels bulk with different PEGDA concentrations (20% in blue, 15% in red and 10% in black). Table S1: Sequence and thermodynamic parameters of the DNA probes used in this study.

Author Contributions: experimental data A.M., T.M.C. and L.R.; conceptualization E.B. and F.C.; writing—original draft preparation, A.M., T.M.C. and E.B; supervision, F.C. and PAN; All authors have read and agreed to the published version of the manuscript."

Conflicts of Interest: "The authors declare no conflict of interest."

References

1. Pluen, A.; Netti, P. A.; Jain, R. K.; Berk, D. A., Diffusion of macromolecules in agarose gels: comparison of linear and globular configurations. Biophysical journal 1999, 77 (1), 542-552.
2. Liu, D.; Kotsmar, C.; Nguyen, F.; Sells, T.; Taylor, N.; Prausnitz, J.; Radke, C., Macromolecule sorption and diffusion in HEMA/MAA hydrogels. Industrial & Engineering Chemistry Research 2013, 52 (50), 18109-18120.
3. Cheng, Y.; Prud'Homme, R. K.; Thomas, J. L., Diffusion of mesoscopic probes in aqueous polymer solutions measured by fluorescence recovery after photobleaching. Macromolecules 2002, 35 (21), 8111-8121.
4. Hoffman, A. S., Hydrogels for biomedical applications. Advanced drug delivery reviews 2012, 64, 18-23.
5. Peppas, N. A.; Moynihan, H. J.; Lucht, L. M., The structure of highly crosslinked poly (2-hydroxyethyl methacrylate) hydrogels. Journal of Biomedical Materials Research Part A 1985, 19 (4), 397-411.
6. Anseth, K. S.; Bowman, C. N.; Brannon-Peppas, L., Mechanical properties of hydrogels and their experimental determination. Biomaterials 1996, 17 (17), 1647-1657.
7. D'Errico, G.; De Lellis, M.; Mangiapia, G.; Tedeschi, A.; Ortona, O.; Fusco, S.; Borzacchiello, A.; Ambrosio, L., Structural and mechanical properties of UV-photo-cross-linked poly (N-vinyl-2-pyrrolidone) hydrogels. Biomacromolecules 2007, 9 (1), 231-240.
8. Hoffman, A.; Schmer, G.; Harris, C.; Kraft, W., Covalent binding of biomolecules to radiation-grafted hydrogels on inert polymer surfaces. ASAIO Journal 1972, 18 (1), 10-16.
9. Zalipsky, S.; Harris, J. M., Introduction to chemistry and biological applications of poly (ethylene glycol). ACS Publications: 1997.
10. Peppas, N. A.; Merrill, E. W., Crosslinked poly (vinyl alcohol) hydrogels as swollen elastic networks. Journal of Applied Polymer Science 1977, 21 (7), 1763-1770.
11. Peppas, N.; Huang, Y.; Torres-Lugo, M.; Ward, J.; Zhang, J., Physicochemical foundations and structural design of hydrogels in medicine and biology. Annual review of biomedical engineering 2000, 2 (1), 9-29.
12. Peppas, N. A.; Keys, K. B.; Torres-Lugo, M.; Lowman, A. M., Poly (ethylene glycol)-containing hydrogels in drug delivery. Journal of controlled release 1999, 62 (1), 81-87.
13. Peppas, N. A.; Hilt, J. Z.; Khademhosseini, A.; Langer, R., Hydrogels in biology and medicine: from molecular principles to bionanotechnology. Advanced materials 2006, 18 (11), 1345-1360.
14. Kopecek, J., Hydrogels: From soft contact lenses and implants to self-assembled nanomaterials. Journal of Polymer Science Part A: Polymer Chemistry 2009, 47 (22), 5929-5946.
15. Yasuda, H.; Peterlin, A.; Colton, C.; Smith, K.; Merrill, E., Permeability of solutes through hydrated polymer membranes. Part III. Theoretical background for the selectivity of dialysis membranes. Macromolecular Chemistry and Physics 1969, 126 (1), 177-186.
16. Peppas, N.; Bures, P.; Leobandung, W.; Ichikawa, H., Hydrogels in pharmaceutical formulations. European journal of pharmaceutics and biopharmaceutics 2000, 50 (1), 27-46.
17. Peppas, N. A.; Khare, A. R., Preparation, structure and diffusional behavior of hydrogels in controlled release. Advanced drug delivery reviews 1993, 11 (1-2), 1-35.
18. Bryant, S. J.; Anseth, K. S., Hydrogel properties influence ECM production by chondrocytes photoencapsulated in poly (ethylene glycol) hydrogels. Journal of Biomedical Materials Research Part A 2002, 59 (1), 63-72.
19. Amsden, B., Solute diffusion in hydrogels.: an examination of the retardation effect. Polymer gels and networks 1998, 6 (1), 13-43.
20. Farnan, D.; Frey, D.; Horvath, C., Surface and pore diffusion in macroporous and gel-filled gigaporous stationary phases for protein chromatography. Journal of Chromatography A 2002, 959 (1-2), 65-73.

21. Farnan, D.; Frey, D. D.; Horvath, C., Intraparticle mass transfer in high-speed chromatography of proteins. Biotechnology progress 1997, 13 (4), 429-439.
22. Peng, C.-C.; Kim, J.; Chauhan, A., Extended delivery of hydrophilic drugs from silicone-hydrogel contact lenses containing vitamin E diffusion barriers. Biomaterials 2010, 31 (14), 4032-4047.
23. Lewus, R. K.; Carta, G., Protein diffusion in charged polyacrylamide gels: visualization and analysis. Journal of Chromatography A 1999, 865 (1-2), 155-168.
24. Lewus, R. K.; Carta, G., Protein transport in constrained anionic hydrogels: Diffusion and boundary-layer mass transfer. Industrial & engineering chemistry research 2001, 40 (6), 1548-1558.
25. Russell, S. M.; Belcher, E. B.; Carta, G., Protein partitioning and transport in supported cationic acrylamide-based hydrogels. AIChE journal 2003, 49 (5), 1168-1177.
26. Russell, S. M.; Carta, G., Multicomponent protein adsorption in supported cationic polyacrylamide hydrogels. AIChE journal 2005, 51 (9), 2469-2480.
27. Flory, P. J., Principles of polymer chemistry. Cornell University Press: 1953.
28. Wallace, M.; Adams, D. J.; Iggo, J. A., Analysis of the mesh size in a supramolecular hydrogel by PFG-NMR spectroscopy. Soft Matter 2013, 9 (22), 5483-5491.
29. Sun, J.; Lyles, B. F.; Yu, K. H.; Weddell, J.; Pople, J.; Hetzer, M.; Kee, D. D.; Russo, P. S., Diffusion of dextran probes in a self-assembled fibrous gel composed of two-dimensional arborols. The Journal of Physical Chemistry B 2008, 112 (1), 29-35.
30. Branco, M. C.; Pochan, D. J.; Wagner, N. J.; Schneider, J. P., Macromolecular diffusion and release from self-assembled β-hairpin peptide hydrogels. Biomaterials 2009, 30 (7), 1339-1347.
31. Cohen, Y.; Avram, L.; Frish, L., Diffusion NMR spectroscopy in supramolecular and combinatorial chemistry: an old parameter—new insights. Angewandte Chemie International Edition 2005, 44 (4), 520-554.
32. Cao, S.; Fu, X.; Wang, N.; Wang, H.; Yang, Y., Release behavior of salicylic acid in supramolecular hydrogels formed by l-phenylalanine derivatives as hydrogelator. International journal of pharmaceutics 2008, 357 (1), 95-99.
33. Scalettar, B. A.; Hearst, J. E.; Klein, M. P., FRAP and FCS studies of self-diffusion and mutual diffusion in entangled DNA solutions. Macromolecules 1989, 22 (12), 4550-4559.
34. Colsenet, R.; Söderman, O.; Mariette, F., Pulsed field gradient NMR study of poly (ethylene glycol) diffusion in whey protein solutions and gels. Macromolecules 2006, 39 (3), 1053-1059.
35. Gao, P.; Fagerness, P. E., Diffusion in HPMC gels. I. Determination of drug and water diffusivity by pulsed-field-gradient spin-echo NMR. Pharmaceutical research 1995, 12 (7), 955-964.
36. Kwak, S.; Lafleur, M., Self-diffusion of macromolecules and macroassemblies in curdlan gels as examined by PFG-SE NMR technique. Colloids and Surfaces A: Physicochemical and Engineering Aspects 2003, 221 (1), 231-242.
37. Gagnon, M.-A.; Lafleur, M., Comparison between nuclear magnetic resonance profiling and the source/sink approach for characterizing drug diffusion in hydrogel matrices. Pharmaceutical development and technology 2011, 16 (6), 651-656.
38. Gagnon, M.-A.; Lafleur, M., Self-diffusion and mutual diffusion of small molecules in high-set curdlan hydrogels studied by 31P NMR. The Journal of Physical Chemistry B 2009, 113 (27), 9084-9091.
39. Escuder, B.; LLusar, M.; Miravet, J. F., Insight on the NMR study of supramolecular gels and its application to monitor molecular recognition on self-assembled fibers. The Journal of organic chemistry 2006, 71 (20), 7747-7752.
40. Shapiro, Y. E., Structure and dynamics of hydrogels and organogels: An NMR spectroscopy approach. Progress in Polymer Science 2011, 36 (9), 1184-1253.
41. Kärger, J., NMR self-diffusion studies in heterogeneous systems. Advances in Colloid and Interface Science 1985, 23, 129-148.
42. McConville, P.; Pope, J., A comparison of water binding and mobility in contact lens hydrogels from NMR measurements of the water self-diffusion coefficient. Polymer 2000, 41 (26), 9081-9088.
43. Zustiak, S. P.; Leach, J. B., Hydrolytically Degradable Poly(Ethylene Glycol) Hydrogel Scaffolds with Tunable Degradation and Mechanical Properties. Biomacromolecules 2010, 11 (5), 1348-1357.
44. Thakur, A.; Wanchoo, R.; Singh, P., Structural parameters and swelling behavior of pH sensitive poly (acrylamide-co-acrylic acid) hydrogels. Chemical and Biochemical Engineering Quarterly 2011, 25 (2), 181-194.
45. Johnson Jr, C. S., Diffusion ordered nuclear magnetic resonance spectroscopy: principles and applications. Progress in Nuclear Magnetic Resonance Spectroscopy 1999, 34 (3-4), 203-256.
46. Holz, M.; Heil, S. R.; Sacco, A., Temperature-dependent self-diffusion coefficients of water and six selected molecular liquids for calibration in accurate 1H NMR PFG measurements. Physical Chemistry Chemical Physics 2000, 2 (20), 4740-4742.
47. Causa, F.; Aliberti, A.; Cusano, A. M.; Battista, E.; Netti, P. A., Supramolecular spectrally encoded microgels with double strand probes for absolute and direct miRNA fluorescence detection at high sensitivity. Journal of the American Chemical Society 2015, 137 (5), 1758-1761.
48. Battista, E.; Mazzarotta, A.; Causa, F.; Cusano, A. M.; Netti, P. A. Core-Shell Microgels with Controlled Structural Properties. Polym. Int. 2016, 65 (7), 747–755. https://doi.org/10.1002/pi.5076.
49. Celetti, G.; Di Natale, C.; Causa, F.; Battista, E.; Netti, P. A. Functionalized Poly(Ethylene Glycol) Diacrylate Microgels by Microfluidics: In Situ Peptide Encapsulation for in Serum Selective Protein Detection. Colloids Surfaces B Biointerfaces 2016, 145, 21–29. https://doi.org/10.1016/j.colsurfb.2016.04.036.
50. Battista, E.; Causa, F.; Netti, P. Bioengineering Microgels and Hydrogel Microparticles for Sensing Biomolecular Targets. Gels 2017, 3 (2), 20. https://doi.org/10.3390/gels3020020.

 doi:10.20944/preprints202106.0264.v1